View metadata, citation and similar papers at core.ac.uk
brought to you by CORE
provided by RERO DOC Digital Library

Eur. Phys. J. D **46**, 9–14 (2008)
DOI: 10.1140/epjd/e2007-00275-5

THE EUROPEAN PHYSICAL JOURNAL D

Lifetime of the Cs $6P_{1/2}$ state in bcc and hcp solid ^{4}He

A. Hofer[1,a], P. Moroshkin[1], S. Ulzega[2], and A. Weis[1]

[1] Département de Physique, Université de Fribourg[b], Chemin du Musée 3, 1700 Fribourg, Switzerland
[2] EPFL, Lausanne, Switzerland

Received 16 May 2007 / Received in final form 4 September 2007
Published online 26 September 2007 – © EDP Sciences, Società Italiana di Fisica, Springer-Verlag 2007

Abstract. We present the first experimental study of time-resolved fluorescence from laser-excited Cs($6P_{1/2}$) atoms isolated in a solid ^{4}He matrix. The results are compared to the predictions of the bubble model including the interaction of the atomic dipole with its radiation reflected at the bubble interface. Our results show that in liquid He as well as in the body-centered cubic (bcc) crystalline phase of He the lifetime of excited Cs atoms does not depend on He pressure, in agreement with our theory. When going from the bcc to the hexagonally close-packed (hcp) phase of ^{4}He the lifetime is reduced by ≈10% and decreases further with increasing He pressure. We assign this effect to the formation of Cs^*He_n exciplexes, and determine the pressure dependence of the probability that the $6P_{1/2}$ state decays via this nonradiative channel.

PACS. 32.70.Cs Oscillator strengths, lifetimes, transition moments – 67.40.Yv Impurities and other defects – 82.20.Xr Quantum effects in rate constants (tunneling, resonances, etc.)

1 Introduction

In recent years the study of metal atoms, and in particular alkali atoms, isolated in condensed ^{4}He matrices [1–4] and in He nanodroplets [5] has become a well established spectroscopic technique. In the past most of the information on the dopants' properties were inferred from spectroscopic experiments involving the study of absorption and emission spectra of laser-induced fluorescence from the near UV to the near IR range of the spectrum as well as from double resonance experiments involving optically detected magnetic resonance induced by rf or microwave radiation. Overviews of the fields are given in the review papers [6] (liquid helium and nano-droplets) and [7] (solid helium). Recent aspects of the dopant spectroscopy in condensed helium and He droplets include the observation of bound states of excited alkali atoms with one or several bound He atoms, so-called exciplexes [7].

No time dependent studies of alkalis in *solid* He have been reported so far, although excited state lifetimes of Rb and Cs immersed in *superfluid* He have been studied in the past [8,9]. Those experiments had revealed some interesting observations: while the Cs $6P_{1/2}$ lifetime was found to be pressure independent up to the solidification point, with a value below the free atomic lifetime, the lifetime of the corresponding $5P_{1/2}$ state of Rb decreases with increasing pressure, leading to a complete quenching of the fluorescence. The authors of [9] interpreted their observations as being due to the formation of exciplexes, a deexcitation channel which opened only for Rb as the corresponding potential barrier for exciplex formation is lower than for Cs.

In this paper we present a first study of pressure dependent lifetimes of the $6P_{1/2}$ state in Cs atoms implanted in the body-centered cubic (bcc) and in the hexagonally close-packed (hcp) phase of solid He. In the bcc phase we find lifetimes which coincide with the ones observed in the liquid phase, while the passage to the hcp phase shows a pronounced jump to lower lifetimes, with a further quenching when the He pressure is increased.

In contrast to He droplets, in which the alkali atoms reside on the droplet surface and quickly desorb after optical excitation, the alkali atoms, when immersed into bulk (liquid or solid) He matrices, are stabilized in small cavities, so-called atomic bubbles. These bubble structures (spherical in bcc, slightly deformed in hcp) can be modelled by the so-called standard bubble model (SBM).

In Section 2 we will recall the main aspects of the standard bubble model (SBM) used to calculate excited state lifetimes. In Section 3 we present the experimental set-up and the lifetime measurements and the results of the measurements are discussed in Section 4.

2 Theory

We have applied the standard bubble model (SBM) [1,10] to describe the bubble structure and the properties of the trapped atom. The SBM treats the He bulk as an incompressible liquid and the bubble shape is described by a

[a] e-mail: adrian.hofer@unifr.ch
[b] www.unifr.ch/physics/frap/

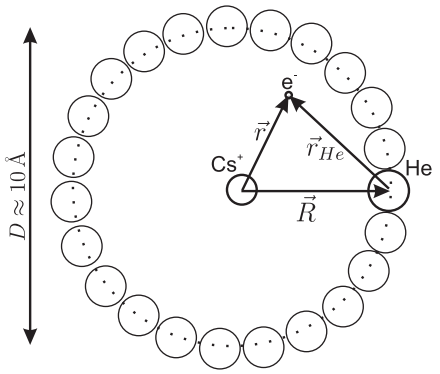

Fig. 1. Ingredients for the calculation of the Cs wavefunctions in a spherical He bubble. The Schrödinger equation is solved for the Cs valence electron moving in the combined potential of the Cs^+ core and the pseudopotential of the surrounding He bulk. The size of the bubble is approximately 10 Å for a ground state Cs atom.

spherical model distribution of the He density. The size of the bubble for a given pressure is obtained by minimizing the total bubble energy whose standard [10] contributions are the pressure-volume energy, the surface tension energy, a kinetic energy contribution related to the density change at the interface and the Cs-He interaction energy.

The latter contribution can be described by a summation of Cs-He pair potentials. Here, however, we take another approach, by solving the Schrödinger equation for the valence electron moving in the potential of the Cs^+ core and a pseudopotential formed by the surrounding He (Fig. 1) [11,12]. A coarse outline of this calculation was given in [13] and was presented with more details in [14]. The main contribution to the interaction of the electron with the core is described by a scaled Thomas-Fermi model potential following the work of Gombas [12] and Norcross [15]. Several corrections, such as the dipolar and quadrupolar core polarizabilities were taken into account.

The radiative lifetime of an excited state with angular momentum J_e and transition frequency ω_0 to the ground state (angular momentum J_g) is related to the transition dipole matrix element via

$$\frac{1}{\tau} = \frac{\omega_0^3}{3\,\pi\,\epsilon_0\,\hbar\,c^3}\frac{1}{2J_e+1}\left|\left\langle n_e L_e J_e \middle\| d \middle\| n_g L_g J_g \right\rangle\right|^2, \qquad (1)$$

where the reduced matrix element is related to the radial integral of the wavefunctions via

$$\begin{aligned}\left|\left\langle n_e L_e J_e \middle\| d \middle\| n_g L_g J_g \right\rangle\right| &= \left|\left\langle 6\mathrm{P}_{1/2} \middle\| d \middle\| 6S_{1/2} \right\rangle\right| \\ &= \sqrt{\frac{2}{3}}\, e \int_0^\infty R_{6S} r^3 R_{6P}\, dr. \qquad (2)\end{aligned}$$

We evaluated the radial integrals numerically using our solutions of the Schrödinger equation. The obtained values for the free Cs atom and for Cs in a spherical He bubble are listed in Table 1, together with the transition wavelengths and the lifetimes. For the free Cs atom we obtain a lifetime which is approximately 4% larger than the precise experimental value of [16,17]. This sets a scale for the precision of our model calculations.

Table 1. Calculated and experimental reduced dipole matrix elements $\langle d \rangle = \langle 6\mathrm{P}_{1/2} \| d \| 6\mathrm{S}_{1/2} \rangle$ in atomic units, transition wavelengths and lifetimes of the free Cs atom and of Cs in a spherical bubble. All results, except for the one in the first line are from the present work.

Sample	$\langle d \rangle$ (ea_0)	λ (nm)	τ (ns)
free Cs atom, exp. [16]	–4.4978(61)	894.6	34.82
free Cs atom, calc.	–4.41	894.3	36.2
Cs in bcc He, exp.	–4.61	884.2	32.5
Cs in bcc He, calc., without cavity effect	–4.33	882.5	35.8
Cs in bcc He, calc., with cavity effect	–4.56	885.9	32.8

We have also calculated the lifetime of the $6\mathrm{P}_{1/2}$ state in spherical He bubbles for pressures covering the superfluid and the solid bcc phase. According to the bubble model the optical excitation to the $6\mathrm{P}_{1/2}$ state occurs in a (small) bubble whose size is determined by the $6\mathrm{S}_{1/2}$ wave function. Once the atom is in the excited state the bubble expands in order to minimize the total energy due to the larger spatial extension of the $6\mathrm{P}_{1/2}$ state. This expansion happens on a much faster time scale than the subsequent fluorescence emission, which occurs in the larger bubble, in which the Cs wavefunctions are less perturbed by the He matrix. The calculated lifetimes τ^{theo} are shown, together with the experimental data, in Figure 4.

As a general trend we observe that the dipole matrix element decreases with increasing He pressure, while the transition frequency ω_0 increases, so that the two changes cancel each other to a large extend. This reflects well the observed independence of the $6\mathrm{P}_{1/2}$ lifetime in pressurized superfluid He [9] and its present extension into the solid bcc phase discussed below.

For a complete description one has to take the interaction of the excited Cs atom with its own electromagnetic radiation reflected at the interface to the (dielectric) helium bulk into account. It is well-known that an oscillating electric dipole close to a dielectric surface induces an oscillating polarization in the dielectric. The interaction between the two dipoles then results in a frequency shift of the emitted light and in a change of its lifetime (real and imaginary parts of the dipole's energy). The latter effect depends on the retardation between the oscillations of the atomic dipole and the reflected electromagnetic field. It may vary considerably and even change sign depending on the thickness of the bubble interface and its refraction index [18]. In order to estimate the influence of the reflected radiation on the observed lifetime of Cs in condensed He we use the results of [18], where an analytic expression is derived for the radiative lifetime of an atom in a spherical nanocavity with a sharp boundary to the outer dielectric bulk. Assuming an index of refraction for solid He of $n_{\mathrm{He}} = 1.0365$ (bcc phase at 1.5 K, 26.6 bar, molar volume 21.1 cm^3) and a bubble radius $R_{\mathrm{b}}(6\mathrm{P}_{1/2}) = 14.0a_0$,

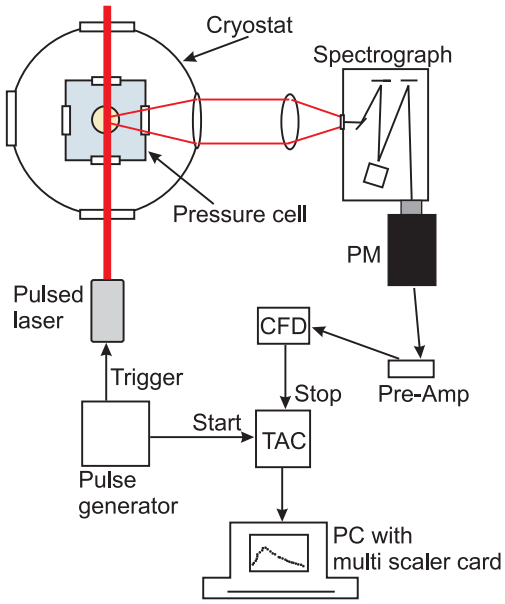

Fig. 2. Set-up for the lifetime measurements. The repetition rate of the excitation laser is 10 kHz. Details are given in the text.

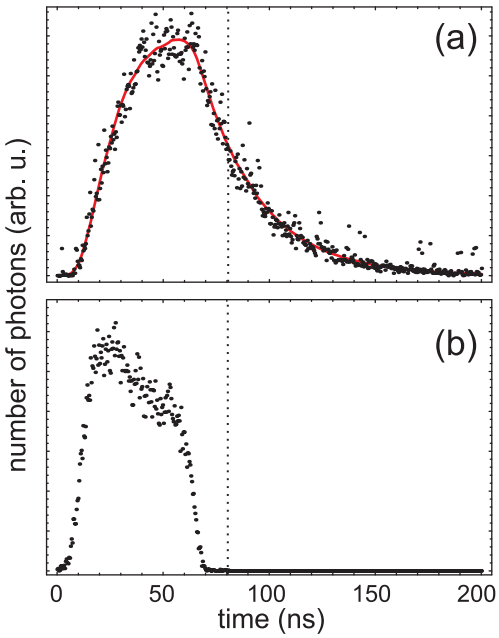

Fig. 3. (Color online) Histogram of arriving photon delay times (dots); (a) shows the decay curve of the $6P_{1/2}$ state of cesium. The solid (red) line is a fit to the experimental points. The fit function is a convoluting of the excitation pulse shape, shown in (b), with an exponential decay $\exp(-t/\tau)$. The vertical dotted line shows the point, where the excitation pulse is off, and from whereon the decay curve in (a) is a pure exponential.

obtained from our bubble calculations [14], we find an enhanced radiative decay rate $\gamma = 1.086\,\gamma_0$, where γ_0 is the uncorrected radiative decay rate of the Cs atom. The lifetime corrected for this cavity effect is given in Table 1.

Note that this dielectric cavity correction was shown previously to contribute to the shift of spectral lines of alkali atoms on He nano-droplets [5].

3 Experiment

3.1 Experimental set-up

The experiments were performed in a Cs doped solid He matrix. Details of the techniques for doping a He crystal were presented in our previous publications [7,19]. A crystal is produced by pressurizing liquid He in a copper cell (170 cm^3 of inner volume) immersed in a liquid He bath cooled to 1.5 K by pumping on its surface. The cell has five windows in three orthogonal directions for optical access. The crystal is doped with Cs atoms by laser ablation using a frequency doubled pulsed Nd:YAG laser (10 mJ pulses) with a repetition rate of ∼3 Hz. The laser beam is focused by a height adjustable lens mounted above the cell onto a solid Cs target located at the bottom of the cell.

The set-up for the lifetime measurements of the atomic $6P_{1/2}$ state of Cs in solid He is shown in Figure 2. A pulsed diode laser at 850 nm (10 kHz repetition rate) was used for the optical excitation of the implanted atoms. The atomic fluorescence light is collected by a lens inside the cryostat and collimated into a direction perpendicular to the laser beam, where it is focused into a grating spectrograph (MS257, Oriel) equipped with a single-photon counting photomultiplier (Burle, model C31034, cooled to –30 °C, 2.5 ns rise-time) mounted after the output slit. The spectrograph suppresses very efficiently scattered laser light, whose wavelength differs by 30 nm from the fluorescence wavelength. The excitation laser is triggered by a pulse generator, a delayed pulse of which is used as a start signal for a time-to-amplitude converter (TAC). The photomultiplier (PM) is operated in the single-photon counting mode. The PM pulses are amplified and analyzed by a constant fraction discriminator (CFD), whose logic output serves as the stop signal for the TAC. The TAC delivers analogue voltage pulses whose amplitudes are proportional to the time delay between the start and stop pulses. A histogram of the amplitudes of the TAC pulses is recorded in 0.4 ns wide time bins using a multiscaling card in a personal computer. This histogram directly reflects the time dependence of the fluorescence intensity. In order to avoid pile-up effects, the light intensity was attenuated in an appropriate way so that on average less than one photon was detected per excitation pulse.

All measurements were done at 1.5 K or 1.6 K, in the pressure range of 26–38 bar, both in the bcc and hcp phase of solid He.

3.2 Life time measurements

A typical time trace of the fluorescence is shown in Figure 3a, while Figure 3b shows the shape of the laser pulse recorded with the same system. The rise of the fluorescence during the laser pulse is taken into account in the

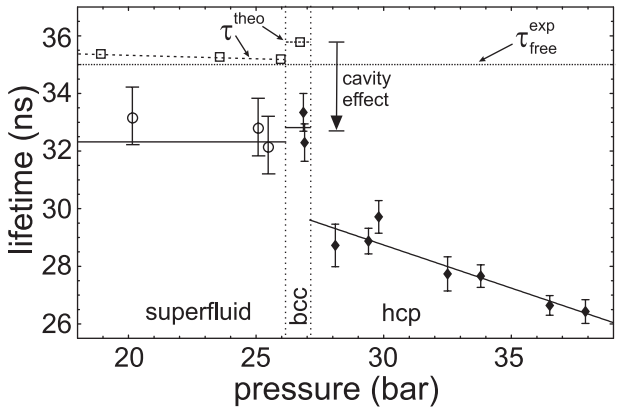

Fig. 4. Pressure dependence of the Cs $6P_{1/2}$ lifetime in solid and liquid He. The open circles are experimental values from [9] and the horizontal solid line through these points represents their average value including points down to zero pressure not shown in the graph. The vertical dotted lines mark different phase boundaries of condensed He. The horizontal dotted line at 34.8 ns indicates the lifetime of the free Cs atom. The open squares are theoretical lifetimes obtained in this work by the SBM. The cavity effect is discussed in the text.

subsequent analysis by fitting a convolution of an exponential decay with the laser pulse shape to the data. In another analysis we determined the decay time by fitting an exponential decay curve to the tail of the signal, where the excitation of Cs atoms no longer interferes with their decay. The two methods yield lifetimes that coincide within 2%, which is on the order of the statistical errors. The values shown in Figure 4 are from the analysis with the convolution method.

We studied the pressure dependence of the lifetime τ of the Cs $6P_{1/2}$ state in the range including both bcc (at 26 bar) and hcp (up to 38 bar) phases of solid He. The results are shown in Figure 4, which also shows lifetimes of the Cs $6P_{1/2}$ measured in superfluid He taken from [9]. The authors of that reference have measured lifetimes of the lowest $nP_{1/2}$ states of Rb and Cs in condensed He from the saturated vapor pressure up to the solidification point at 25 bar. For Cs they found a lifetime of approximately 32.3 ns, which is nearly independent on the helium pressure, while the lifetimes in Rb decrease in a dramatic way with increasing pressure, leading to a complete quenching of the fluorescence at the solidification pressure. Here we find that the lifetimes of Cs in the bcc phase coincide with the (pressure independent) values in liquid He. When increasing the He pressure beyond the bcc phase we first observe a pronounced jump by 3.2(9) ns to shorter lifetimes at the bcc–hcp phase transition, and then a further decrease of the lifetime with increasing He pressure at a rate of –0.30(6) ns/bar.

4 Discussion

4.1 Lifetimes in the bcc phase

The experimental lifetime values obtained in the bcc phase of the He matrix are close to the ones measured previously in liquid He. Our theoretical calculation in the frame of the SBM (presented in Sect. 2) yields a value $\tau^{\rm theo}$ in the bcc phase of 35.8 ns at $T = 1.5$ K and $p = 26.6$ bar. If we apply the correction due to the interaction of the atomic dipole with the surrounding dielectric He bulk (cavity effect), discussed in the theory section we obtain $\tau = 35.8/1.086 = 33.0$ ns, in excellent agreement with the experimental value $\tau = 32.8(9)$ ns (average of the two data points in bcc). Because of the pressure independence of the lifetimes, this correction (the index of refraction of liquid He ($n_{\rm He} = 1.0365$) is close to the one of solid bcc He) also leads to an agreement between the experimental lifetimes [9] and our theoretical values in superfluid He. However, this good agreement has to be taken with some caution, considering that our wavefunctions for the free Cs atom reproduce the experimental lifetime of the free atom $\tau^{\rm exp}_{free} = 34.8$ ns only at a level of 4%. Nevertheless it seems that we have strong evidence that the alteration by the dielectric cavity gives an important contribution to the lifetime of excited Cs atoms in superfluid and bcc solid He.

4.2 Lifetimes in the hcp phase

As can be seen in Figure 4 the pressure dependence of the lifetime makes an abrupt jump of –3.2(9) ns at the bcc–hcp phase transition. The SBM cannot account for this discontinuity. Moreover, the lifetimes show a pronounced pressure dependence in the hcp phase, another fact which the SBM cannot explain; the SBM calculations predict a change of τ by approximately –0.5 ns when increasing the pressure from 27 to 34 bar, whereas the experimental lifetime changes by approximately –1.6 ns over that range.

We assign the increased deexcitation rate in the hcp phase to the morphological change of the atomic bubble structure from a spherical shape in the bcc matrix to an elliptically deformed bubble in the uniaxial hcp matrix. Experimental evidence for such bubble deformations were presented earlier based on optical and magnetic resonance experiments (a review of those experiments is given in [7]). It seems that this structural change opens a new deexcitation channel for the $6P_{1/2}$ state which most likely consists in the formation of Cs^*He_2 and Cs^*He_N ($N = 6$ or 7) exciplexes. Recently we have performed a detailed spectroscopic study of such exciplexes [4] which fluoresce at a strongly red-shifted wavelength, not detected in our present set-up.

Cs-He exciplex formation has not been observed in liquid nor in bcc He when the Cs atoms are excited at the D_1 transition, while Rb-He exciplexes were observed under similar conditions in Rb-doped liquid He [20]. For both Rb and Cs the exciplex formation after D_1 excitation involves the tunneling of He atoms through a potential barrier V_0 [4]. It is known [9,4] that the potential barrier is lower for Rb than for Cs, so that the density of pressurized liquid He is sufficient for a significant formation of exciplexes during the lifetime of the $5P_{1/2}$ state. This is nicely illustrated by the He pressure-dependent

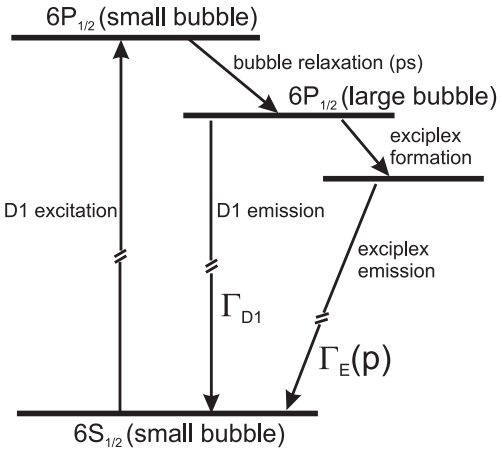

Fig. 5. Decay channels of the $6P_{1/2}$ state of Cs in solid He following atomic D_1 absorption at 850 nm. The excitation takes place in a small bubble which relaxes towards a larger bubble with a lower energy. The excited atom in the larger bubble can decay to the ground state either via atomic D_1 emission (at 880 nm) or via exciplex formation and subsequent exciplex fluorescence. Figure is not to scale with the energy levels.

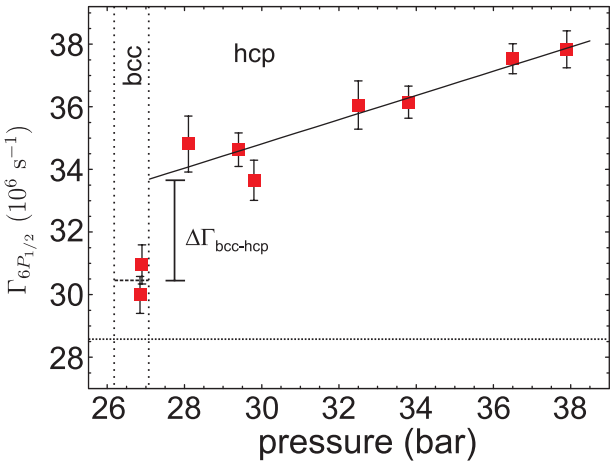

Fig. 6. Decay rate of the $6P_{1/2}$ state as a function of pressure. The solid line is a fit to data points using the model of equation (7). The horizontal dotted line indicates the radiative decay rate of the free Cs atom.

fluorescence quenching of Rb in HeII, resulting in a complete disappearance of the Rb fluorescence even before the liquid-bcc phase transition is reached [9]. An increase of the pressure reduces the bubble size and thereby lowers the effective barrier height, so that the tunneling probability increases with He pressure. This general feature explains the pressure dependent decrease of atomic Rb fluorescence in liquid He and of atomic Cs fluorescence in hcp solid He. With the lower barrier height of Rb the exciplex formation thus starts already in the superfluid phase, while with Cs one needs the higher density, and more importantly, the change of symmetry of the trapping site in the solid hcp phase for observing the quenching by exciplex formation.

4.3 Analysis

The diagram in Figure 5 shows the two concurring deexcitation channels of the $6P_{1/2}$ state after D_1 excitation at 850 nm. The two processes can be modeled in terms of decay rates by writing the total $6P_{1/2}$ state decay rate in hcp as

$$\Gamma_{6P_{1/2}} = \Gamma_{D1} + \Gamma_E(p) \quad (3)$$
$$= \Gamma_{D1} + kW_T, \quad (4)$$

where $\Gamma_{D1} = \tau_{D1}^{-1}$, $\Gamma_E(p)$ is the exciplex formation rate, and k is the rate of collisions with the potential barrier for exciplex formation [4]. The probability (Gamov factor) to tunnel through the barrier is

$$W_T = \exp\left[-2\,b\sqrt{\frac{2m}{\hbar^2}(V_0 - E)}\right] \quad (5)$$

where we have assumed for simplicity a square potential of height V_0 and width b. If we assume that the effective barrier height $V_0 - E$ and the barrier width b have a small linear variation with helium pressure p_{He}, the decay rate can be written as

$$\Gamma_{6P_{1/2}} = \Gamma_{D1} + \Delta\Gamma_{bcc-hcp}\exp\left[\alpha(p_{He} - p_{bcc-hcp})\right] \quad (6)$$
$$\approx \Gamma_{D1} + \Delta\Gamma_{bcc-hcp} + \beta(p_{He} - p_{bcc-hcp}), \quad (7)$$

where $p_{bcc-hcp}$ is the pressure at the bcc–hcp phase transition, and where $\Delta\Gamma_{bcc-hcp}$ is the jump of the decay rate at the bcc–hcp phase boundary, if we take the radiative lifetimes in the bcc and in the hcp phases to be identical. The experimental value of $\Delta\Gamma_{bcc-hcp}$ is $+3.2(9)\times10^6$ s^{-1}. Figure 6 shows the total decay rate of the $6P_{1/2}$ state as a function of pressure. The function of equation (7) is fitted to the data points and shown as a solid line. The fit yields $\beta = 0.38(7)\times10^6$ s^{-1}bar^{-1}.

From equation (7) we can derive the branching ratio to the exciplex channel, i.e., the probability for the $6P_{1/2}$ state to form an exciplex to be

$$W_{exci} = \frac{\Gamma_E(p)}{\Gamma_E(p) + 1/\tau_{D1}}$$
$$= \frac{\Delta\Gamma_{bcc-hcp} + \beta\,(p_{He} - p_{bcc-hcp})}{\Delta\Gamma_{bcc-hcp} + \beta\,(p_{He} - p_{bcc-hcp}) + 1/\tau_{D1}}. \quad (8)$$

Figure 7 shows the pressure dependence of the branching ratio W_{exci}.

As discussed in Section 4.2 the barrier height V_0 prevents exciplex formation in the bcc phase. The jump of the exciplex formation rate at the bcc-hcp phase transition can thus be explained by a lowering of the effective potential barrier. This effect can be explained by the slightly smaller bubble size and morphological change of the bubble shape in hcp by which the He atoms at the bubble interface are brought closer to the top of the barrier.

The absolute value of the effective barrier height $V_0 - E$ cannot be inferred from the present data since we do not know the collision rate with the barrier, which depends on the oscillation frequency of the interface atoms, nor details

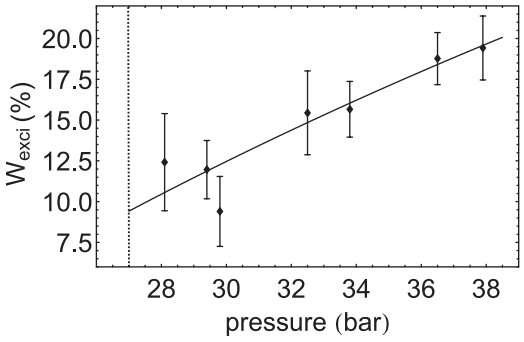

Fig. 7. Exciplex formation probability $W_{\rm exci}$ as a function of pressure. The vertical dashed line marks the pressure of the bcc to hcp phase transition.

of the barrier shape. As discussed in [4] the ro-vibrational structure of the final bound exciplex allows, in principle, for a resonant tunneling to occur, whenever E matches a ro-vibrational eigenstate of the exciplex. Such processes might show up as resonant changes in the pressure dependence of the atomic lifetimes.

4.4 Summary

We have presented a detailed experimental study of the pressure dependence of the Cs $6P_{1/2}$ state lifetime in bcc and hcp solid He. The standard bubble model was used to estimate the lifetime of the $6P_{1/2}$ state in superfluid He and in bcc solid He. It reproduces well the pressure independence of the lifetimes in pressurized superfluid He and in the bcc phase. The absolute value predicted by the model is 9% larger than the measured one. We explain this discrepancy by a reduction of the lifetime due to the interaction of the atomic dipole with its mirror images in the dielectric (cavity effect). In the uniaxial hcp phase the observed pressure dependence of the lifetime can be explained by the opening of an additional deexcitation channel which consists in the formation of Cs^*He_2 and Cs^*He_N ($N = 6$ or 7) exciplexes. We suggest that the jump of the lifetime at the bcc-hcp phase transition may be explained by the structural change of the atomic bubble in hcp ^{4}He. The experimental data were used to infer the pressure dependent probability of exciplex formation.

This work was supported by the grant number 200021-111941/1 of the Schweizerischer Nationalfonds.

References

1. T. Kinoshita, K. Fukuda, Y. Takahashi, T. Yabuzaki, Phys. Rev. A **52**, 2707 (1995)
2. T. Kinoshita, K. Fukuda, T. Yabuzaki, Phys. Rev. B **54**, 6600 (1996)
3. S. Kanorsky, A. Weis, M. Arndt, R. Dziewior, T.W. Hänsch, Z. Phys. B **98**, 371 (1995)
4. P. Moroshkin, A. Hofer, D. Nettels, S. Ulzega, A. Weis, J. Chem. Phys. **124**, 024511 (2006)
5. F. Stienkemeier, J. Higgins, C. Callegari, S.I. Kanorsky, W.E. Ernst, G. Scoles, Z. Phys. D **38**, 253 (1996)
6. J.P. Toennies, A.F. Vilesov, Annu. Rev. Phys. Chem. **49**, 1 (1998)
7. P. Moroshkin, A. Hofer, S. Ulzega, A. Weis, Fiz. Nizk. Temp. **32**, 1297 (2006) [Low Temp. Phys. **32**, 981 (2006)]
8. Q. Hui, J.L. Persson, J.H.M. Beijersbergen, M. Takami, Z. Phys. B **98**, 353 (1995)
9. T. Kinoshita, K. Fukuda, T. Matsuura, T. Yabuzaki, Phys. Rev. A **53**, 4054 (1996)
10. S.I. Kanorsky, M. Arndt, R. Dziewior, A. Weis, T.W. Hänsch, Phys. Rev. B **50**, 6296 (1994)
11. J. Pascale, Phys. Rev. A **28**, 632 (1983)
12. P. Gombas, *Pseudopotentiale* (Springer-Verlag, Berlin-Gottingen-Heidelberg, 1956)
13. A. Weis, *Atoms in nanocavities* (Kluwer Academic Publisher, 1995), Vol. 314
14. A. Hofer, P. Moroshkin, S. Ulzega, D. Nettels, R. Müller-Siebert, A. Weis, Phys. Rev. A **76**, 022502 (2007)
15. D.W. Norcross, Phys. Rev. A **7**, 606 (1973)
16. R.J. Rafac, C.E. Tanner, A.E. Livingston, K.W. Kukla, H.G. Berry, C.A. Kurtz, Phys. Rev. A **50**, 1976 (1994)
17. R.J. Rafac, C.E. Tanner, A.E. Livingston, H.G. Berry, Phys. Rev. A **60**, 3648 (1999)
18. V.V. Klimov, V.S. Letokhov, Chem. Phys. Lett. **301**, 441 (1999)
19. M. Arndt, R. Dziewior, S. Kanorsky, A. Weis, T.W. Hänsch, Z. Phys. B **98**, 377 (1995)
20. K. Hirano, K. Enomoto, M. Kumakura, Y. Takahashi, T. Yabuzaki, Phys. Rev. A **68**, 012722 (2003)